

PSEUDOELASTICITY OF $D0_3$ ORDERED MONOCRYSTALLINE Fe_3Al

S. Kabra,¹ H. Bei,^{1,3} D. W. Brown,² M.A.M. Bourke,² and E. P. George,^{1,3}

¹The University of Tennessee, Department of Materials Science and Engineering, Knoxville, TN 37996

²Los Alamos National Laboratory, Los Alamos, NM 87545

³Oak Ridge National Laboratory, Metals and Ceramics Division, Oak Ridge, TN 37831

ABSTRACT

Pseudoelasticity in monocrystalline Fe_3Al (23 at.% Al) was investigated by room-temperature mechanical testing along the $\langle 418 \rangle$ tensile and compressive axes. In tension, up to ~10% strain is recoverable whereas only ~5% strain is recoverable in compression. Straight, parallel, surface step lines were seen to appear/disappear as the specimens were pseudoelastically loaded/unloaded. In contrast, in the plastic region ($\epsilon > 10\%$), wavy slip lines appeared on the specimen surfaces which did not disappear upon unloading. In-situ neutron diffraction was performed during compressive straining and the intensities of several diffraction peaks increase/decrease reversibly during loading/unloading. These changes are consistent with a deformation twin which produces large crystal rotations. They could also be indicative of a phase transformation. Unfortunately, we were able to sample only a limited range of 2θ in the present investigation and, within this range, none of the new peaks that appeared during the pseudoelastic deformation were disallowed peaks for the $D0_3$ crystal structure. Therefore we are unable at this time to distinguish between the two possible mechanisms, twinning and phase transformation.

INTRODUCTION

Iron aluminides based on Fe_3Al have attractive properties for structural applications at intermediate temperatures, including good oxidation resistance and low density, e.g. [1]. However, a property that has gone relatively unnoticed is its room-temperature pseudoelasticity. Pseudoelasticity in single crystal Fe_3Al was reported by Guedou et. al. [2] as early as 1976; however, there have been relatively few papers since then regarding this phenomenon [2-9]. Briefly, pseudoelasticity is observed only for compositions in the range 21-29 at.% Al [2] and for $D0_3$ rather than B2 ordering [3]. Up to ~5% compressive strain is recoverable, but there is a strong orientation dependence with full recovery possible only for deformation along directions near the $\langle 419 \rangle$ that maximize the Schmid factor for the (101)[111] system, and significantly less recovery as one deviates from this orientation [8]. When the alloy is deformed at 77 K, the imposed strain does not recover upon unloading but does so only after the specimen warms up to room temperature [2,3], indicating that Fe_3Al exhibits both shape memory behavior and pseudoelasticity.

At first, twinning was suggested as a possible mechanism for pseudoelasticity [3], but no supporting experimental evidence was offered. Subsequently, an APB-dragging mechanism was postulated [4], which seemed to be supported by in-situ transmission electron microscopy observations showing reversible motion of the leading partial dislocation during loading/unloading [4,7-9]. However, it is difficult to see how large amounts of strain can be produced by the APB mechanism if only the leading partial moves while the trailing partial remains fixed. On the other hand, if the entire dislocation moves (and multiplies), enough strain can certainly be generated, but then there is no restoring force to drive the strain recovery during unloading.

In the most widely studied system that exhibits both pseudoelasticity and shape memory, NiTi, a stress-induced martensitic transformation is known to be responsible for

pseudoelasticity [e.g., 10]. While there have been no reports of such a transformation in Fe_3Al , it may be because, to our knowledge, there have been no attempts to perform in-situ structural characterization during deformation.

In this study we first investigate pseudoelasticity in tension (since prior experiments were done in compression) and compare our results with the earlier compression data. We also performed in-situ neutron diffraction during compressive loading/unloading to determine whether any structural transformations occur during the pseudoelastic deformation.

EXPERIMENTAL DETAILS

Alloys of composition Fe-23Al (all compositions in at.%) were arc melted, drop-cast, and directionally solidified in an optical floating zone furnace to produce a $\langle 100 \rangle$ single crystal. This single crystal was oriented and cut normal to $\langle 418 \rangle$ and used to seed additional single crystals having the $\langle 418 \rangle$ growth direction. The $\langle 418 \rangle$ crystals were homogenized at 1100°C for 48 h and furnace cooled at 80°C/h to maximize $D0_3$ order [9].

Dogbone shaped specimens having a $1 \times 2 \times 24$ (mm) gage section were tensile tested along $\langle 418 \rangle$ direction at room temperature at a constant crosshead speed of 0.001 mm/s, which corresponded to an engineering strain rate in our specimens of $5 \times 10^{-5} \text{ s}^{-1}$.

In-situ neutron diffraction experiments were performed on the SMARTS diffractometer at the Lujan Center for Neutron Scattering at the Los Alamos National Laboratory [11]. Compressive loading-unloading cycles were performed on cylindrical specimens 6 mm in diameter and 14.4 mm long with their compression axes along $\langle 418 \rangle$. At various points on the stress-strain curve, the cross-head motion was stopped (for ~ 3 minutes) to collect diffraction data.

RESULTS AND DISCUSSION

Figure 1 shows tensile stress-strain curves of Fe_3Al exhibiting almost complete recovery of applied strains up to $\sim 10\%$ and plastic (unrecoverable) deformation beyond that. There is no indication of any hardening in tension, unlike in compression where there is a small amount of hardening evident in the pseudoelastic regime (Fig. 2). Another difference between tension and compression is that significantly more strain is recovered in tension than in compression. The elastic to pseudoelastic transition occurs at a stress of ~ 500 MPa in both tension and compression and there is a large loading/unloading hysteresis.

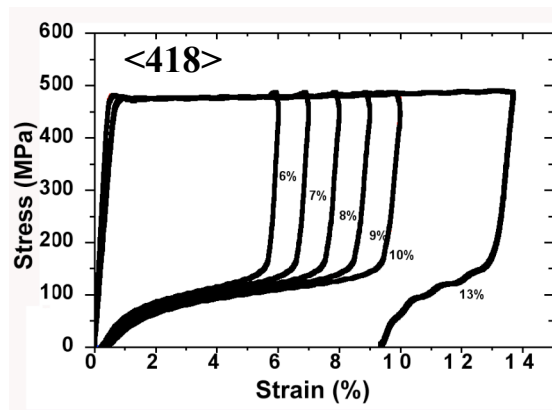


Figure 1 Tensile stress-strain curves of monocrystalline Fe_3Al .

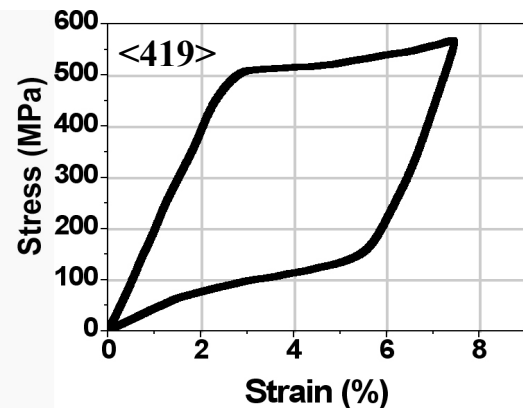


Figure 2 Compressive stress-strain curve of monocrystalline Fe_3Al [9].

Most of the applied strain (~97%) was recovered immediately upon unloading [Fig. 3 (a)]. The remaining strain recovered in a time-dependent manner, as shown in the inset of Fig. 3 (a) for 10% applied strain, and in Fig. 3 (b) for other strains. Straight, parallel, step lines appeared on the sample surfaces in the pseudoelastic region [Fig. 4 (a)], and their density increased with increasing strain. Upon unloading from the pseudoelastic region these lines disappeared completely [Fig. 4 (b)].

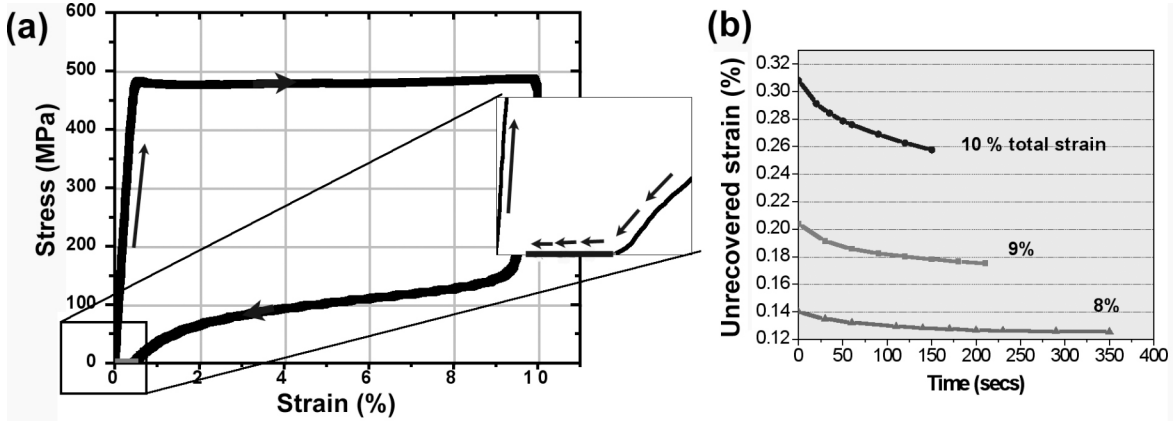


Figure 3 (a) Tensile stress-strain curve showing that ~97% of the applied strain of 10% is recovered instantaneously upon unloading with the remainder recovered in a time-dependent manner; (b) time dependence of strain recovery after unloading.

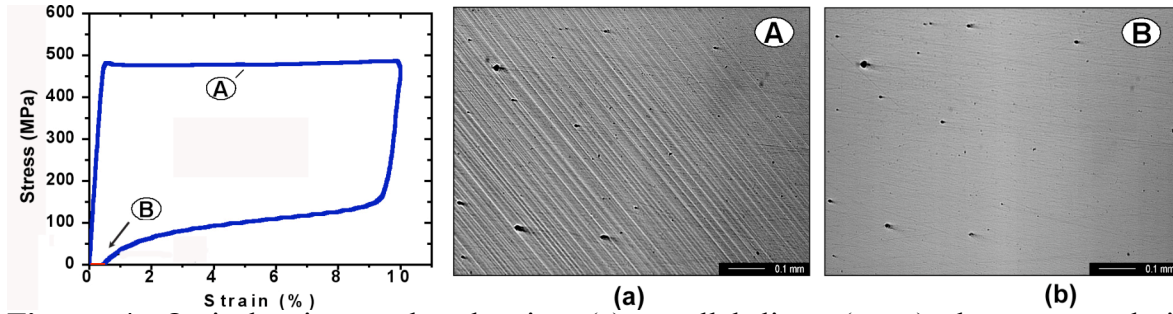


Figure 4. Optical micrographs showing (a) parallel lines (steps) that appear during pseudoelastic deformation, and (b) the complete disappearance of these surface steps upon unloading.

When specimens were loaded in tension to strains more than 10%, a large part of the strain was unrecoverable upon unloading (Fig. 1). This result can be related to the two types of surface features that appear during loading. Figure 5 (a) shows parallel step like features (Type 1 lines) that appear on the surface of the specimen when it is deformed in the pseudoelastic region [similar to Fig. 4 (a)]. After ~10% strain, wavy slip lines (Type 2 lines) appear on the surface [Fig. 5 (b)]. Upon unloading from ~13% strain, most, but not all, of the Type 1 lines disappear, whereas all the Type 2 lines remain [Fig. 5 (c)]. Clearly, Type 1 lines are associated with the recoverable part of the strain while Type 2 lines are slip lines associated with plastic deformation. Only ~4% strain is recovered when the sample is unloaded from 13% strain, whereas essentially all of the strain is recovered when the sample is unloaded from 10% strain (within the pseudoelastic regime). This indicates that a major part of the pseudoelastic (recoverable) strain is trapped once irreversible plastic deformation commences.

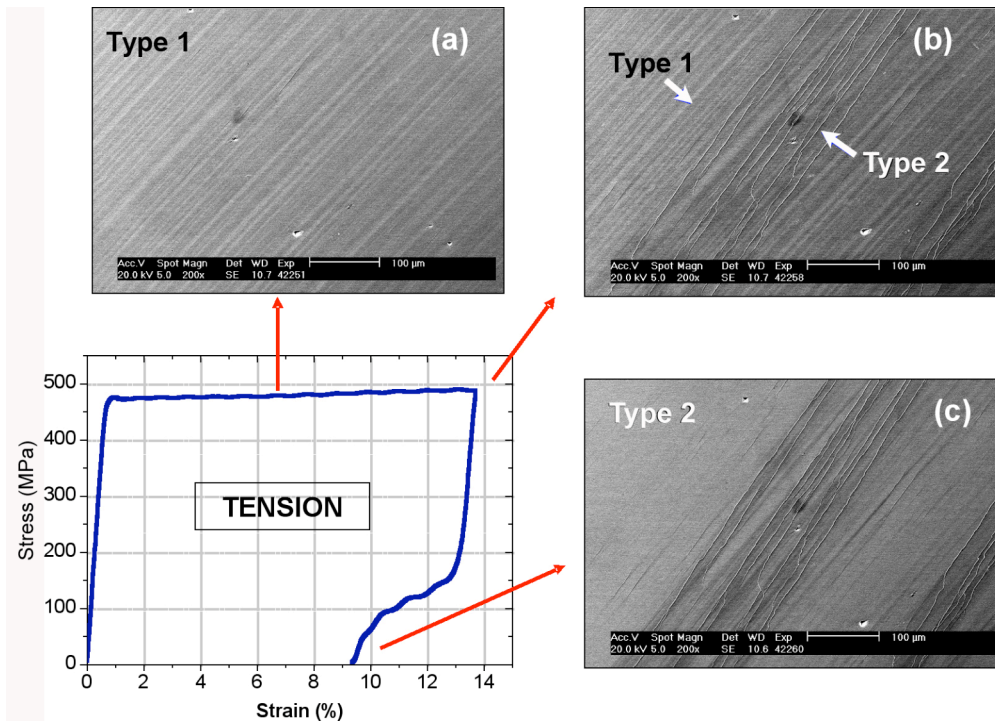


Figure 5 SEM micrographs showing (a) surface steps (Type 1 lines) in the pseudoelastic region, (b) wavy slip lines (Type 2 lines) beyond $\sim 10\%$ applied strain, and (c) Type 2 lines remaining after unloading (many, but not all, of the Type 1 lines are gone).

Neutron diffraction patterns were obtained during loading/unloading in compression along $\langle 418 \rangle$. Figure 6 (a) shows the stress-strain curves for two such cycles. In the first cycle the specimen was deformed in the pseudoelastic regime ($\sim 3\%$ maximum strain), while in the second cycle the specimen was taken into the plastic regime ($\sim 6\%$ maximum strain). As mentioned before, the recoverable strain in compression [Fig. 6 (a)] is considerably less than that in tension (Fig. 1). Neutron diffraction patterns were obtained while the cross-head was stopped at different positions [some of which are indicated by arrows in Fig. 6 (a)].

Figure 6 (b) shows the diffraction patterns obtained at four positions (1, 2, 3 and 4) on the stress-strain curve. Position 1 lies well within the elastic region of the stress-strain curve and the diffraction pattern at this position is essentially the same as that in the unloaded condition (Position 3). Large changes in peak intensity with respect to the initial pattern are evident in the pseudoelastic region (Position 2). Some peaks increase in intensity, while others decrease. Two of the notable peaks are (422) and (844): they have zero intensity in position 1 but have significant intensity at position 2. In fact, the (422) peak goes from zero intensity before straining (1), to being the most intense peak in the pseudoelastic region (2), and back to zero intensity in the unloaded condition (3). Such changes in peak intensity are indicative of large crystal rotations, which may be caused by stress-induced twinning or a change in crystal symmetry due to a stress-induced phase transformation. Unfortunately, the detector configuration in our current experiments allowed us to sample only a limited range of 2θ . Within this range, none of the new peaks that appeared at position 2 are disallowed peaks for the $D0_3$ crystal structure. Therefore we are unable at this time to distinguish between the two possible mechanisms. Additional experiments are planned using more complete detector coverage that will allow us to measure a larger portion of the standard stereograph of the material. Figure 6 (b) also shows a spectrum obtained at position 4, (i.e. after the specimen

was unloaded from the plastic region). Unlike what was observed at position 3, the intensities of the (422) and (844) peaks do not go to zero at position 4, indicating that a significant portion of the previously recoverable (pseudoelastic) strain gets trapped and becomes unrecoverable once plastic deformation commences, consistent with the behavior of the Type 1 and 2 surface features discussed earlier (Fig. 5).

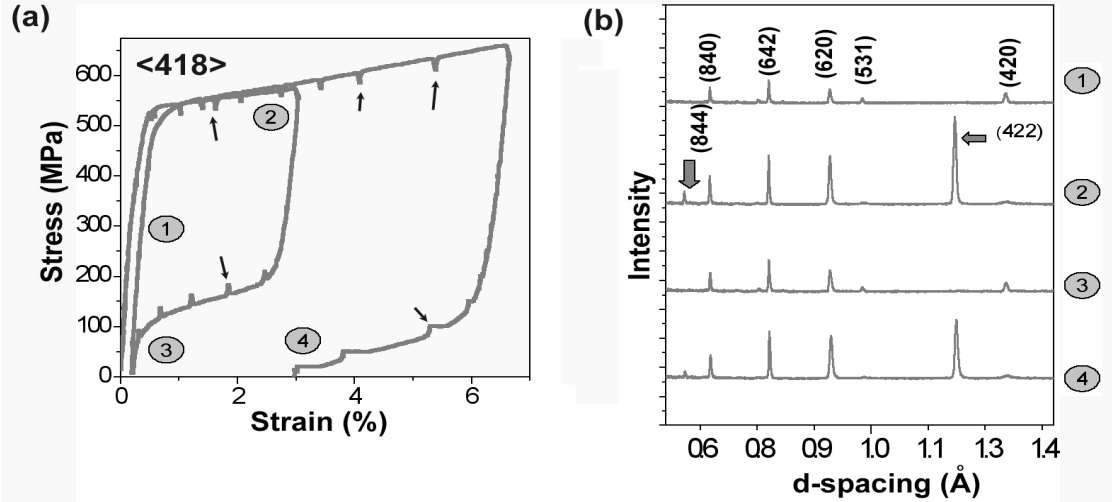


Figure 6 (a) Compressive stress-strain curves of Fe₃Al single crystal, (b) neutron diffraction patterns obtained at different locations (1, 2, 3, and 4) on the stress-strain curves.

Figure 7 (a) shows the variation of the (422) peak intensity as a function of the applied strain. In the elastic region ($\epsilon < 0.5\%$), the (422) peak is not present. It makes its first appearance in the pseudoelastic region, and thereafter increases in intensity almost linearly with increasing strain. Upon unloading, its intensity decreases with decreasing strain, following to the loading curve but with a small hysteresis. The normalized (422) peak intensity can also be plotted as a function of applied stress, and compared with the stress-strain behavior as shown in Fig. 7 (b). There is an almost one-to-one correlation between the two curves.

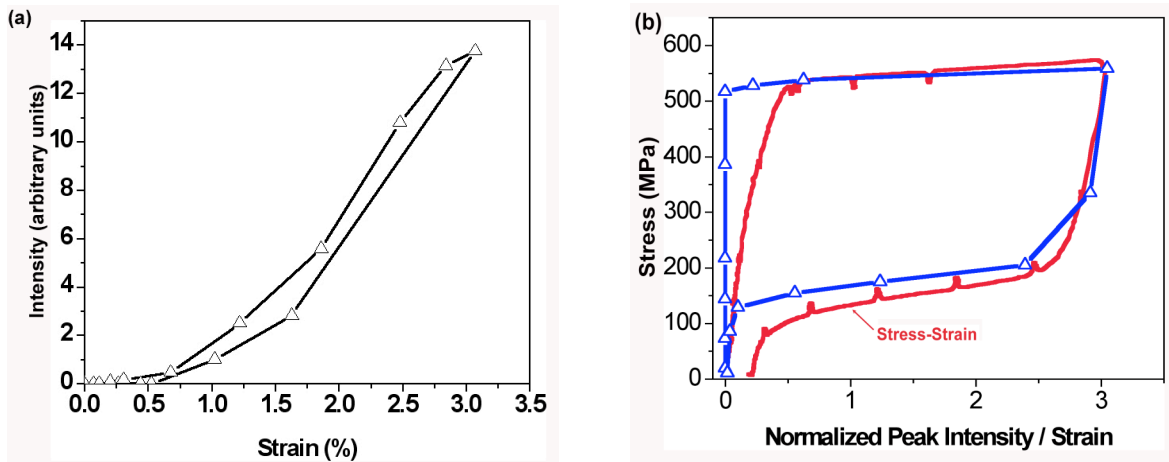


Figure 7 (a) Peak intensity of (422) reflections as a function of applied strain; (b) Variation of the normalized (422) peak intensity with stress compared to the pseudoelastic stress-strain behavior.

CONCLUSIONS

Single crystal Fe₃Al can recover up to 10% strain in tension along <418>, almost twice as much as previously shown to be recoverable in compression. In conjunction with this recoverable strain, straight, parallel step lines appeared on the specimen surface, which disappeared upon unloading. Beyond ~10% strain, plastic deformation set in and wavy slip lines appeared on the surface which did not disappear upon unloading. In-situ neutron diffraction performed during compressive straining showed that the intensities of several diffraction peaks changed reversibly during loading/unloading, most notably the (422) peak which went from zero intensity before straining, to being the most intense peak in the pseudoelastic region, and back to zero intensity after unloading. Such changes in peak intensity are indicative of large crystal rotations, which may be caused by stress-induced twinning. They may also be indicative of a stress-induced phase transformation. Unfortunately, the detector configuration in our current experiments allowed us to sample only a limited range of 2θ . Within this range, none of the new peaks that appeared during the pseudoelastic deformation are disallowed peaks for the $D0_3$ crystal structure. Therefore we are unable at this time to distinguish between the two possible mechanisms, twinning and phase transformation.

ACKNOWLEDGMENTS

Research sponsored by the Division of Materials Sciences and Engineering, Office of Basic Energy Sciences, U. S. Department of Energy, under Contract DE-AC05-00OR22725 with UT-Battelle, LLC. This work also benefited from the use of the Los Alamos Neutron Science Center (LANSCE) at the Los Alamos National Laboratory funded by the US Department of Energy under Contract W-7405-ENG-36.

REFERENCES

1. C.G. McKamey, J.H. DeVan, P.F. Tortorelli and V.K. Sikka, *J. Mater. Res.* 6, 1779 (1991).
2. J.Y. Guedou, M. Paliard, J. Rieu, *Scripta Met.* 10, 631 (1976).
3. J.Y. Guedou, J. Rieu, *Scripta Met.* 12, 927 (1978).
4. L.P. Kubin, A. Fourdeux, J.Y. Guedou, J. Rieu, *Phil. Mag. A* 46, 357 (1982).
5. G.I. Nosova, N.A. Polyakova, Ye. Ye. Novikova, *Phys. Met. Metall.* 61, 151 (1986).
6. A. Brinck, C. Engelke, H. Neuhäuser, *Scripta Mater.* 37(5), 569 (1997).
7. E. Langmaack, E. Nembach, *Phil. Mag. A* 79, 2359 (1999).
8. H.Y. Yasuda, K. Nakano, M. Ueda, Y. Umakoshi, *Mat. Sci. Forum* 426-432, 1801 (2003).
9. H.Y. Yasuda, K. Nakano, T. Nakajima, M. Ueda, Y. Umakoshi, *Acta Mater.* 51, 5101 (2003).
10. K. Otsuka, C.M. Wayman, "Shape memory materials", Cambridge University Press, New York, 1998.
11. M. A.M. Bourke, D. C. Dunand, and E. Ustundag, *Applied Physics A* 74, s1707 (2002).